

## Electronic properties of organic monolayers and molecular devices

D VUILLAUME<sup>1</sup>, S LENFANT<sup>1</sup>, D GUERIN<sup>1</sup>, C DELERUE<sup>1</sup>, C PETIT<sup>2</sup>  
and G SALACE<sup>3</sup>

<sup>1</sup>Institut d'Electronique, de Micro-electronique et de Nanotechnologie, CNRS, Molecular Nanostructures and Devices Group, BP69, Avenue Poincaré, 59652 Villeneuve d'Ascq Cedex, France

<sup>2</sup>Centre de Recherche en Sciences et Technologies de l'Information et de la Communication, Université de Reims, BP 1039, 51687 Reims Cedex 2, France

<sup>3</sup>Laboratoire de Microscopies et d'Etudes de Nanostructures, Université de Reims, BP 1039, 51687 Reims Cedex 2, France

E-mail: dominique.vuillaume@iemn.univ-lille1.fr

**Abstract.** We review some of our recent experimental results on charge transport in organic nanostructures such as self-assembled monolayer and monolayers of organic semiconductors. We describe a molecular rectifying junction made from a sequential self-assembly on silicon. These devices exhibit a marked current–voltage rectification behavior due to resonant transport between the Si conduction band and the  $\pi$  molecule highest occupied molecular orbital of the  $\pi$  molecule. We discuss the role of metal Fermi level pinning in the current–voltage behavior of these molecular junctions. We also discuss some recent insights on the inelastic electron tunneling behavior of Si/alkyl chain/metal junctions.

**Keywords.** Molecular electronics; self-assembly.

**PACS Nos** 85.65.+h; 81.07.Nb

### 1. Introduction

As microelectronic devices approach their technological and physical limits [1,2], molecular electronics, i.e. the molecule-based information technology at the molecular scale, becomes more and more investigated and envisioned as a promising candidate for the nanoelectronics of the future. From this respect, supramolecular assembly of organic molecules on solid substrates is a powerful ‘bottom-up’ approach for the fabrication of devices for molecular-scale electronics. The first approach to build an organized assembly of molecules is the Langmuir–Blodgett (LB) method. Many groups have reported on the electrical properties of LB mono- and multilayers for device applications since early works in the 1970s (see a review in [3]). For instance, the most recent and stimulating results to date are the observation of a current rectification behavior through LB monolayers of hexadecylquinolinium

tricyanoquinodimethanide [4–10] and the fabrication of molecular switches based on LB monolayers of catenanes [11–15] although the actual role of molecules in the latter case is still under debate [16,17]. A second method is based on the self-assembly of monolayers of organic molecules on solid substrates (SAM) [3]. Many reports in the literature concern SAMs of thiol-terminated molecules chemisorbed on gold surfaces. For instance, Bumm and coworkers [18,19] studied the conductivity of molecular wires by inserting a few molecules of di(phenylene-ethynylene)benzenethiolate in a SAM of dodecanethiols (which are insulating molecules). The conductivity was investigated using the tip of a scanning tunneling microscope (STM). Kergueris and coworkers [20] repeated these experiments for thiolterthiophene molecules, another prototype of molecular wire. Chemisorbing the two ends of dithiol-based molecules onto two electrodes to form a metal/molecules/metal (MMM) junction can also be investigated. Reed and coworkers [21], Kergueris and coworkers [22] and Weber and coworkers [23,24] used mechanical break junctions to fabricate and to study some MMM junctions based on small oligomer molecules. Chen and coworkers [25,26] used nanopores, in which a small number of molecules are chemisorbed, to fabricate these MMM junctions. With this nanopore configuration, they observed that molecules with a nitroamine redox center (2'-amino-4,4'-di(ethynylphenyl)-5'-nitro-1-benzenethiol) exhibit a negative differential resistance behavior. They also demonstrated the feasibility of a molecular random access memory cell [27]. The switching behavior of these compounds inserted in an alkanethiol SAM was also observed by STM [28] but the respective role of the molecule and chemical link between the molecule and the metal surface is presently a matter of debate [29]. Besides these studies (and others of similar nature) using SAMs on gold electrodes, it is valuable to develop and investigate molecular-scale devices based on SAMs chemisorbed on semiconductors, especially silicon. Silicon is the most widely used semiconductor in microelectronics and a broad family of organic molecules can be grafted on its surface, which opens the possibility of tailoring the surface (modifying the surface potential, for instance) [30–32] for new and improved hybrid molecular/silicon devices. Between the end of the silicon road-map and the envisioned advent of fully molecular-scale electronics, there is, for sure, a role to be played by such hybrid-electronic devices [2,33]. The use of thiol-based SAMs on gold in molecular-scale electronics is supported by a wide range of experimental results on their growth, structural and electrical properties (see the recent review by Schreider [34]). Conversely, SAMs on silicon and silicon dioxide surfaces have proved more difficult to control; large variations were observed from sample-to-sample and from lab-to-lab. Therefore, there were much fewer attempts to use these SAMs in molecular-scale electronics than for the thiol/gold system. Since the first adsorption from solution of alkyltrichlorosilane molecules on a solid substrate (mainly oxidized silicon) introduced by Bigelow *et al* [35] and later developed by Maoz and Sagiv [36], further detailed studies [37–40] have led to a better understanding of the basic chemical and thermodynamical mechanisms of this self-assembly process. Based on this knowledge, we have fabricated SAMs on silicon that are physically and chemically robust, we revisited [41,42] some electronic properties of alkylsilane SAMs, previously analyzed by Mann and Kuhn [43] and Polymeropoulos and Sagiv [44], and we developed nanometer-scale devices using these SAMs [45,46]. SAMs of redox molecules (metallophorphyrines, ferrocene) have also been used as

molecular memories [47,48] in hybrid CMOS/molecular DRAM circuits [49]. Molecular resonant tunneling diodes on silicon have been also demonstrated [50].

Recently [51], we demonstrated a molecular rectifying junction (MRJ) by attaching a donor group (phenyl or thiophene) to the alkyl spacer chain by a sequential grafting on silicon. We obtained rectification ratios up to 35. We showed that the rectification mechanism is a resonance through the molecular orbital of the  $\pi$  group (ascribed to the highest occupied molecular orbital – HOMO) in good agreement with calculations and internal photoemission spectroscopy. This approach allowed us to fabricate molecular rectifying diodes compatible with silicon nanotechnologies for future hybrid circuitries. In this paper, we review the extension of this work to a large number of chemically different  $\pi$  end-groups. We chose a large number of  $\pi$ -groups having different energy levels of their molecular orbitals in gas phase. We start with simple benzyl alcohol and 3-thiophenemethanol. Then, we move from monomers to oligomers: terthiophene and quaterthiophene and to fused oligoacenes: anthracene and pyrene. Our motivations are to establish a relationship between the electrical properties (electronic structure) of the starting  $\pi$  molecules first in vacuum, then when chemisorbed on the silicon substrate and finally the current–voltage rectification behavior of the Si/molecules/metal junctions. From an engineering point of view, the knowledge of this relationship is mandatory to design MRJ with an electrical behavior suitable for device and circuit applications. For instance, in classical semiconductor p–n junctions the threshold voltage for rectification is adjusted by doping, whereas here it is envisioned to do this using chemistry, by changing the nature of the  $\pi$ -group. We discuss the role of Fermi level pinning at the molecule/metal interface in these molecular rectifying junctions.

In the second part of this review, we discuss some results on the electron–molecular vibration interactions measured by inelastic electron tunneling spectroscopy (IETS) in Si/SiO<sub>x</sub>/alkyl/metal junctions [52]. We show that a silicon-based tunnel junction is a suitable test-bed for studying inelastic transport phenomena in organic self-assembled monolayers. The most important molecular vibrations are identified and compared with recent similar IETS investigations on metal/alkyl/metal junctions and with IR, Raman and HREELS data. We have observed that vibronic couplings in the organic tunnel monolayer are more intense than in the SiO<sub>2</sub> tunnel junctions.

## **2. Molecular rectifying diodes**

Experimental and theoretical studies of charge transport in molecular devices are a subject of growing interest [53] in molecular-scale electronics. Charge transfer and band lineup (i.e. the energy position of the molecular orbitals (MOs) with respect to the Fermi energy of the electrodes) are the key parameters controlling the electronic properties in molecular devices [54–57]. This topic has been theoretically addressed [54–57] in ideal metal/molecules/metal junctions with simple molecules (phenyldithiol, alkyl, alkane and phenylethynylene). At the metal/organic semiconductor contact (as in organic light emitting diodes), the breakdown of the vacuum alignment rule (Schottky–Mott model) has been a major discovery to explain the electronic properties of these devices [58,59], and a large number of organic molecules deposited in ultra-high vacuum (UHV) on metal surfaces have been

analyzed [58,59]. It was also established that monolayers of molecules bearing a dipole moment can modify the electron affinity of semiconductor surfaces and consequently the metal/semiconductor Schottky barrier height [60–62]. On the contrary, reports on molecular-scale junctions are scarce, probably because of a smaller number of investigated molecules and metal surfaces (much of the works focused on gold surface with linear alkanes and linear  $\pi$ -conjugated oligomers). Moreover, in molecular junctions, the molecules are generally chemisorbed from solution or from gas phase instead of being UHV deposited.

In this paper, we theoretically and experimentally study the band lineup in a molecular rectifying junction (MRJ). Our device consists of a silicon/ molecules/metal junction in which a  $\pi$ -group has a spatial asymmetric position between the electrodes, since it is grafted on silicon through an alkyl spacer chain. We have shown (for two simple  $\pi$ -groups: phenyl and thiophene) [51] that this device exhibits a marked current–voltage rectification behavior due to a resonant transport between the Si conduction band (CB) and the  $\pi$  highest occupied molecular orbital (HOMO). Thus, the rectification behavior of this junction, e.g. the threshold voltage for rectification, should be sensitive to the nature of the  $\pi$ -group, through the energy position of its MOs with respect to Fermi energies of the electrodes ( $E_{\text{FM}}$  for the metal and  $E_{\text{FSi}}$  for Si). This MRJ is used here as a tool for probing band lineup in molecular-scale junctions made of various  $\pi$ -groups: phenyl, anthracene, pyrene, ethylenedioxythiophene (EDT), ethylenedioxybenzene (EDB), thiophene, terthiophene (3T) and quaterthiophene (4T) (figure 1). The charge transport properties and the electronic structures of these MRJs are electrically characterized and compared with self-consistent tight-binding (SC-TB) calculations of the semiconductor–molecule junction. We clearly establish that the Fermi level pinning at the metal/ $\pi$ -group interface plays a key role in the electrical behavior of these MRJs.

Self-assembled monolayers (SAMs) of n-alkenyl-trichlorosilane ( $\text{SiCl}_3-(\text{CH}_2)_n-\text{CH}=\text{CH}_2$  with  $n = 6-15$ ) are chemisorbed from solution on  $n^+$ -type (resistivity of  $\sim 10^{-3} \Omega\cdot\text{cm}$ ) silicon wafers covered by its native oxide according to silanization protocols described in [41,51,63,64]. We graft  $\pi$ -conjugated moieties onto the previously formed SAMs [51,64]. Figure 1 shows a schematic representation of these SAMs. The details of the SAM synthesis and their physical characterizations (water contact angle, ellipsometry, infra-red spectroscopy) are given elsewhere [64]. We form the MRJ by evaporating the metal (aluminum, 200–300 nm thick) through a shadow mask (electrode area:  $10^{-2} \text{ mm}^2$ ) using an ultra-high vacuum (UHV)  $e$ -beam evaporation system. A yield (of about 50–70% ratio of nonshort-circuited devices over  $>20$  measured devices per  $\pi$ -group) is obtained. Aluminum (instead of Au) is chosen to avoid any rectification effect coming from the difference in the work functions of the two electrodes (4.2 eV for Al and 4.1 eV for  $n^+$ -type Si, electron affinity in the latter case,  $E_{\text{FM}} \sim E_{\text{FSi}}$ ) [65].

The electronic structures of the silicon/molecules junctions are calculated by SC-TB method. We consider a model system characterized by a two-dimensional periodicity, with the Si substrate modeled by a slab containing nine layers of Si atoms. The conformation of the molecules is determined by energy minimization using the semiempirical method PM3 (parametric method 3). Then, the molecule is attached directly on one Si surface atom through a Si–C bond. We passivate all

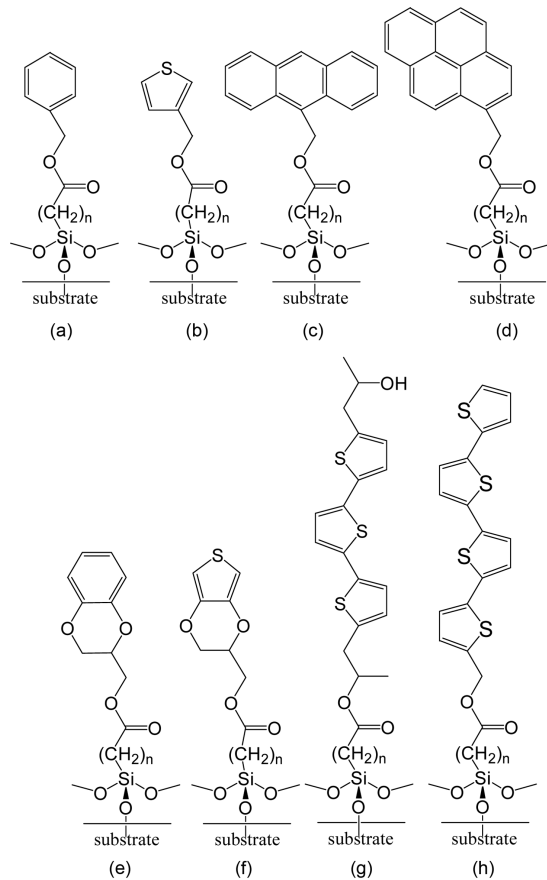


**Figure 1.** Schematic view of the SAMs with different  $\pi$ -groups: phenyl (a), thiophene (b), anthracene (c), pyrene (d), ethylenedioxybenzene (EDB) (e), ethylenedioxythiophene (EDT) (f), terthiophene (3T) (g), and quaterthiophene (4T) (h).

other dangling bonds at the Si surfaces by hydrogen. The molecule is set with the long axis of its alkyl chain in the all-trans conformation perpendicular to the surface. The size of the unit cell is large enough to avoid chemical interaction between the molecules. From the PM3 calculations, we also derive the dipole moment, the HOMO and LUMO (lowest unoccupied molecular orbital) of the isolated molecule. Details of SC-TB technique and parameters for the molecules are given elsewhere [66,67]. We have not included the SiO<sub>2</sub> layer in these calculations because we have shown elsewhere [42] that the position of the MOs with respect to the Si band structure is only weakly influenced by the SiO<sub>2</sub> layer. Note, that the metal electrode is not included in these calculations. Figure 2 shows the calculated density of states (DoS) for several  $\pi$ -groups. We determine the energy position of the LUMO and HOMO of these  $\pi$ -groups with respect to  $E_{\text{FSi}}$  (here at the Si-CB for the n<sup>+</sup>-Si), or equivalently to  $E_{\text{FM}}$  ( $E_{\text{FM}} \sim E_{\text{FSi}}$ ). We use the bare Si electron affinity

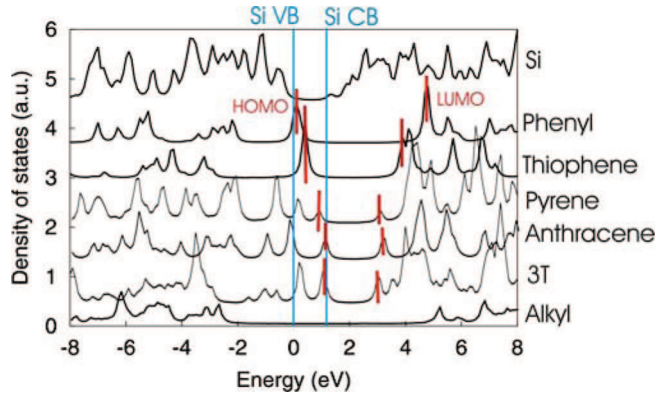


**Figure 2.** Calculated density of states (DoS) in the silicon substrate (top), in the alkyl chain (bottom) and in different  $\pi$ -groups. The long lines indicate the position of the bottom of the Si conduction band (CB) and top of the Si valence band (VB) and the short lines are the position of the HOMO and LUMO of the  $\pi$ -groups (zero energy is taken at the top of Si-VB).

because it was shown [68] that this value is not changed by more than  $\sim 200$  meV for Si substrates functionalized by SAMs with dipole moments of the same order of magnitude as for the molecules used in the present work ( $< 3$  D, PM3 calculations). This value is on a par with the accuracy of the MOs determined in this work (see below and error bars in figure 4).

The rectification effect arises for a negative bias applied on the Al electrode because the energy difference between  $E_{\text{FSi}}$  and the HOMO is lower than that with the LUMO [51]. Consequently a lower threshold (in absolute value) is required to have a resonance between the Si-CB and the HOMO when applying a negative bias on the metal electrode than between the Si-CB and the LUMO for a positive bias. Thus, the threshold voltage for rectification,  $V_T$ , is related to the energy difference,  $E_0$ , between the HOMO and the Si-CB of the  $n^+$ -Si,  $V_T \approx E_0/e\eta$  (i.e.  $\sim -E_0/e$  since  $\eta$  is  $\sim 1$ ) [51],  $e$  is the electron charge. According to DoS calculations (figure 2),  $V_T$  is expected to vary by about 1 V since the HOMO level moves from Si-VB (valence band) to Si-CB depending on the  $\pi$ -group. Figure 3 shows current-density vs. voltage curves ( $J$ - $V$ ) for the MRJs. All junctions exhibited the current rectification, which was not observed through a monolayer without  $\pi$ -group (Si- $n^+$ /alkyl/Al junctions) [41,42,51]. However,  $V_T$  [69] does not depend on the nature of the  $\pi$ -group (inset of figure 3),  $V_T \sim -0.6 - -0.7$  V. Since the current transport is dominated by a resonant effect through the HOMO, we fitted (solid lines in figure 3) the  $J$ - $V$  curves by a one-level model, with  $E_0$  as the fitting parameter [70,71]:

$$J = \frac{2J_0}{\pi} \left\{ \tan^{-1}[\theta(|E_0| + \eta eV)] - \tan^{-1}[\theta(|E_0| - (1 - \eta)eV)] \right\}, \quad (1)$$

where  $V$  is the applied potential on the metal electrode,  $e$  is the electron charge,  $\eta$  is the fraction of the potential seen by the  $\pi$  moiety,  $J_0$  is the saturation current and  $\theta$  is the electrode/molecule coupling parameter. The  $\eta$  values ( $\sim 0.83$  to  $\sim 0.9$  depending on the alkyl chain length) were estimated using simple dielectric model

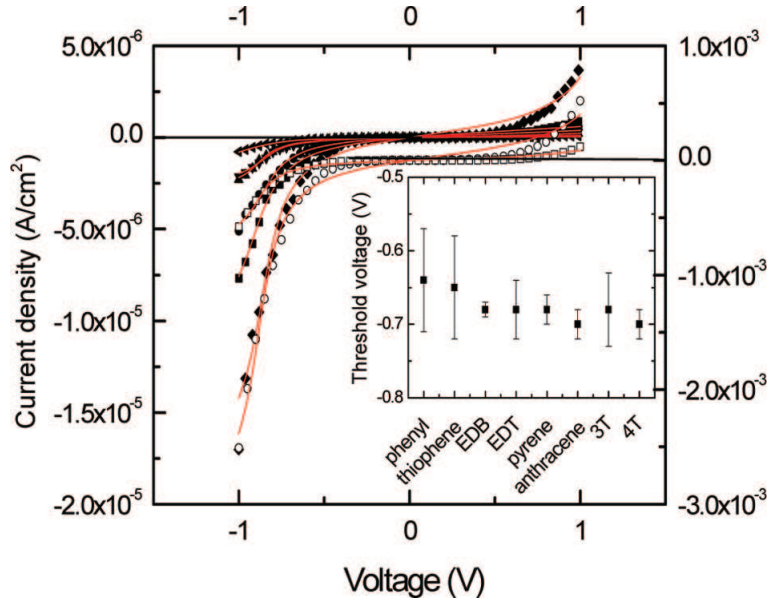


**Figure 3.** Typical current density–voltage characteristics of the MRJs. Left scale: MRJs with  $(\text{CH}_2)_{15}$  alkyl chains terminated by phenyl (■), pyrene (●), thiophene (◆), anthracene (▲), EDT (▼), and EDB (◄). Right scale: MRJs with  $(\text{CH}_2)_6$  alkyl chains terminated by 3T (□), and 4T (○). Solid lines are fits by eq. (1). Inset: Variation of  $V_T$  vs. the  $\pi$ -groups. The error bars are the FWHM (full-width half-maximum) of the statistical data distribution obtained on a large number ( $>20$ ) of devices for each  $\pi$ -group.

for the potential distribution within the molecule [51]. Figure 4 summarizes the experimental position of the HOMO deduced from the averaged  $E_0$  values for all the fitted curves. We also plot the calculated HOMO level of the  $\pi$ -group attached to Si substrate through the alkyl chain as deduced from the DoS in figure 2.

Except for the phenyl and thiophene, the experimental results do not follow the theoretical expectations (figure 4). From our experiments, the HOMO of the  $\pi$ -groups is always at about 0.75–0.8 eV below the Si-CB, or in other words, the metal Fermi energy level is pinned at about 0.75–0.8 eV above the HOMO (figure 4). We deduced that an organic/metal interface dipole shifts down the HOMO level of the  $\pi$ -groups by  $\Delta \sim 0.75$ ,  $\sim 0.58$ ,  $\sim 0.51$ ,  $\sim 0.75$ ,  $\sim 0.81$  and  $\sim 0.62$  eV, for EDB, EDT, pyrene, anthracene, 3T and 4T end-groups, respectively. This dipole corresponds to a charge transfer,  $n = (\epsilon_0 \epsilon_i \Delta A_{\text{mol}} / \delta e^2)$ , ranging from  $\sim 2 \times 10^{-2}$  to  $\sim 0.2$  electron/molecule from the SAM towards the metal electrode, with  $\epsilon_0$  the vacuum dielectric constant,  $\epsilon_i$  the dielectric constant of the organic/metal interface region (we assume the same value as for the SAM,  $\epsilon_i \sim 2.5\text{--}3$  [64]),  $A_{\text{mol}}$  the area per molecule ( $\sim 30\text{--}50 \text{ \AA}^2$ , depending on the  $\pi$ -groups), and  $\delta$  the thickness of the interfacial layer (estimated as the distance between the center of mass of the  $\pi$ -group and the metal surface, from  $\sim 3 \text{ \AA}$  to  $\sim 10 \text{ \AA}$  depending on the molecules). This also corresponds to a dipole momentum,  $\mu = n\delta$ , between  $\sim 0.3$  and  $\sim 9.5$

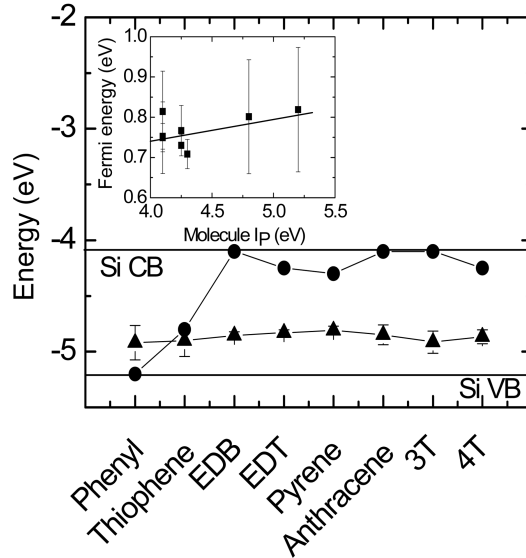


**Figure 4.** Energy position of the HOMO level (vacuum level as the zero energy reference) for several  $\pi$ -groups as deduced from SC-TB calculations ( $\bullet$ ), and from the fit of eq. (1) ( $\blacktriangle$ ) on the experimental results. The error bars are the FWHM (full-width half-maximum) as in figure 3. Inset: Metal Fermi energy position (with respect to the HOMO of the  $\pi$ -group) vs.  $I_P$  of the  $\pi$ -group. The plotted value corresponds to  $-E_0$  where  $E_0$  is determined from the fit of eq. (1) on the  $J$ - $V$  curves.  $I_P$  (calculated by SC-TB) is the absolute value with respect to the vacuum level. The line is a linear fit with a slope of  $\sim 0.04 \pm 0.04$ .

Debye. A usual way to quantify the Fermi level pinning is to calculate the so-called interface slope parameter,  $S = |dE_F/dW_M|$ , where  $W_M$  is the metal work function. Here, since we used only one metal and various organic molecules, one can equivalently determine,  $S = |dE_F/dI_P|$ , where  $I_P$  is the ionization potential of the molecule.  $S = 1$  corresponds to the Schottky–Mott model [72,73] and  $S = 0$  to the Bardeen [74] model. From the plot of  $E_F$  vs.  $I_P$  (figure 4, inset) we deduced an average slope  $S = 0.04 \pm 0.04$ . This slope is related to the density of interface states at the Fermi level,  $D_{it}(E_F)$  by [75] as  $D_{it} = \varepsilon_0 \varepsilon_i (1 - S) / e^2 \delta S$ . With the estimates used for  $\varepsilon_i$  and  $\delta$  to calculate the dipole moment (see above), we derived  $D_{it}(E_F)$  in the range  $\sim 3 \times 10^{14}$  to  $\sim 10^{15} \text{ cm}^{-2} \text{ eV}^{-1}$ .

The Fermi level pinning can be due to metal-induced gap states (MIGS) as in the usual inorganic semiconductor/metal interface [76,77]. Recently, MIGS at metal/organic interfaces has been theoretically and experimentally studied in PTCDA/Au [78]. The creation of MIGS results in a pinning of the metal Fermi level very near the charge neutrality level (CNL), i.e. the energy position for which the total charge integrated over the band-gap density is null. In our case, another likely origin of the metal Fermi pinning is the creation of chemically-induced gap states (CIGS) at the metal/monolayer interface due to the possible chemical reaction of aluminum with the  $\pi$ -conjugated moieties [58]. It was shown that

Al reacts with oxygen-based terminal groups such as  $-\text{COOH}$ ,  $-\text{CO}_2\text{CH}_3$ ,  $-\text{OH}$ ,  $-\text{OCH}_3$  forming organoaluminum complexes [79–83]. However, reports on vapor deposition of metals on SAMs bearing a conjugated end-group are scarce. Ahn and Whitten [84] have observed by X-ray photoemission spectroscopy a strong chemical interaction between vapor-deposited Al and a thiophene-terminated SAM. De Boer *et al* reported (infra-red spectroscopy) that Al atoms reacted with the conjugated backbone of thiol-oligophenyl SAMs on gold. Thus, it is likely that Al chemically reacts with any of the eight  $\pi$ -groups used in this work, or even with the ester group if some Al atoms penetrate into the SAMs. In addition, it is also likely that Al atoms can react with residual oxygen in the vacuum chamber during deposition, forming a very thin, even uncompleted, aluminum oxide layer between the SAM and the Al electrode. Both these mechanisms are probably responsible for the high density of metal-induced gap states and Fermi level pinning in these MRJs. From a theoretical point of view, more calculations are in progress to determine the electronic structure of the whole Si/molecule/metal junction which requires an exact treatment of the metal/organic chemical reactions and interface dipoles [78,85].

### 3. Inelastic tunneling through alkyl chains

These last years, the electronic properties of organic self-assembled monolayers (SAMs) have been more and more investigated in order to be used in future microelectronics devices [41,45,46]. Recently, SAMs of saturated alkyl chains have been demonstrated to produce very good insulating ultra-thin layers [41,86]. To reduce the gate insulator thickness below 3 nm, SAMs of alkyl chains have been successfully used in both silicon and organic transistors [45,46,87]. Organic materials are attractive for making low-cost electronic devices, as light emitting diode and transistor for use in flexible displays.

Recently, Kushmerick *et al* [88] and Wang *et al* [89] have reported low-temperature charge transport measurements of metal/molecules/metal (MMM) junctions and have investigated, by IETS, the electron–molecular vibration coupling in insulating alkyl chains and in  $\pi$ -conjugated molecular wires. Moreover, theoretically incoherent electron–molecular vibration scattering has been investigated and computed in octane-thiolate sandwich by first principles density functional theory (DFT) calculations [90]. Understanding vibronic interactions between electrons and nuclear motions in molecules is a key point in molecular electronic devices [53].

In this paper, we investigate electron–molecular vibration coupling in SAMs using the metal-oxide–silicon (MOS) tunnel junctions as a test-bed. The SAMs are included in the MOS tunnel junction by chemisorption onto the ultra-thin  $\text{SiO}_2$  layer before evaporating the aluminum gate.

The Al/SAM/ $\text{SiO}_2$ / $\text{Si}(n^+)$  (100) are prepared from highly-doped silicon in order to have a metallic behavior. The preparation of the ultra-thin thermal dioxide films and evaporation of the aluminum gate (300 nm in thickness) are described in [91]. The SAMs constituted of alkyl chains of eight carbon atoms are prepared by chemisorption in solution of octyl-1-enyl-trichlorosilane as described elsewhere [41,63]. The thickness of these SAMs is measured by ellipsometry and found to

be equal to 1.7 nm. The structural and molecular organizations of the SAMs are analyzed by contact angle measurements, infra-red spectroscopy, ellipsometry and atomic force microscopy to check that they are ordered and densely packed [63]. An aluminum electrode (area of  $10^{-2}$  cm<sup>2</sup>) is gently evaporated through a shadow mask to complete the junction. Organic monolayers are prone to suffer from metallic filamentary conduction pathway upon metal evaporation. A low deposition rate (0.1–0.5 Å·s<sup>-1</sup>) and a large distance (70 cm) between the sample (held at a constant temperature of 20°C) and the crucible are used to reduce damages on the SAM. A yield of about 50–70% (ratio of non-short-circuited devices over total measured ones) is obtained for our molecular junctions. Generally, current densities in the range of  $10^{-4}$  to  $10^{-3}$  A/cm<sup>2</sup> are measured at the bias voltage of 1 V. These current densities are comparable to those in MMM junctions [89].

The IET spectra are performed at liquid helium temperature (4.2 K). These spectra are obtained by measuring the second derivatives of the tunneling current through the junction by a lock-in amplifier technique, with an AC modulation signal ( $f = 893$  Hz,  $V_\omega = 2\text{--}5$  mV) and a slowly varying DC voltage applied to the junction [92]. The DC bias ramp is obtained from a digital-to-analog converter.

The full-width at half-maximum (FWHM) of the line peak  $\delta V_{\text{exp}}$  is given by

$$\delta V_{\text{exp}} = \sqrt{(5.44kT)^2 + (1.22eV_\omega)^2 + (\delta V_{\text{nat}})^2}, \quad (2)$$

where  $5.44kT$  [93] is the thermal broadening,  $1.22eV_\omega$  [94], the modulation broadening and  $\delta V_{\text{nat}}$  the natural line width. In our experiments, we find  $\delta V_{\text{nat}}$  of about 2 mV, and  $\delta V_{\text{exp}}$  about 4.8 mV for  $T = 4.2$  K and  $V_\omega = 2$  mV [95]. The cryogenics technique is described in our previous paper [91] and the experimental set-up in recent specific papers [92,96].

Figure 5 shows an IET spectrum after background removal in an energy range from 0 to 300 meV (0 to 2420 cm<sup>-1</sup>), obtained by averaging several scans from an Al/SiO<sub>2</sub>/Si (n<sup>+</sup>) junction on the Si(111) orientation.

Three regions with specific infra-red vibration modes can be distinguished:

1. In the energy range 35–80 meV (282.3–645.2 cm<sup>-1</sup>), strong structures that correspond to phonons in the Si substrate [95].
2. In the range 130–180 meV (1048.4–1451.7 cm<sup>-1</sup>), a smaller band structure corresponding to the phonons of the SiO<sub>2</sub> barrier.
3. In the other ranges of energy (80–130 meV (645.2–1048.7 cm<sup>-1</sup>), and higher than 180 meV), small structures sometimes attributed to molecular vibrations present in the tunnel barrier [91].

Figure 6 shows the IET spectrum of an Al/SAM/SiO<sub>2</sub>/Si(n<sup>+</sup>) (100) junction. This tunnel spectrum has been obtained seven times with an excellent reproducibility. We observed in the energy range 10 to 65 meV (80.6 to 524.6 cm<sup>-1</sup>), the Si phonon peaks. Above this energy range, we have observed several large peaks belonging to the alkyl chain in the SAM. The largest peaks represent increase of ~1% in the junction conductance, less than the strong silicon phonon structures (6%) in MOS structure [91] but of the same order of magnitude as molecular vibrations in MIM junctions [97]. Based on previous IR, Raman and high resolution electron energy loss spectroscopy (HREELS), we are able to reasonably assign the most intense vibration modes of the alkyl chains.

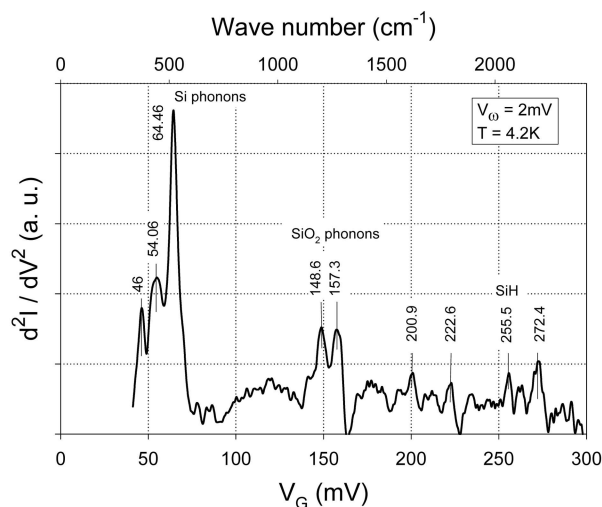


Figure 5. IET spectrum of a Al/SiO<sub>2</sub>/Si(n<sup>+</sup>) junction.

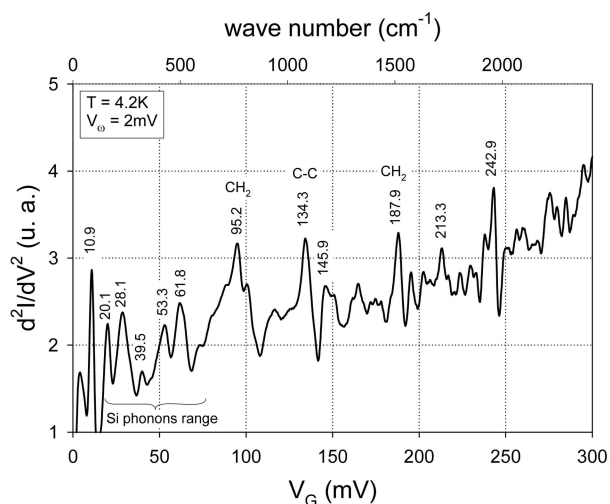


Figure 6. IET spectrum of a Al/SAM/SiO<sub>2</sub>/Si(n<sup>+</sup>) junction.

Beyond the silicon phonon spectrum energy, we can mainly observe four important peaks:

1. The  $\delta$ -CH<sub>2</sub> rocking mode at 95.2 meV (767.8 cm<sup>-1</sup>). This first assignation is in agreement (95 mV) with Raman data [98] and has been also recently found independently by Wang *et al* [89] and by Kushmerick *et al* [88] in the IETS of alkanedithiol SAMs. In our case, the intensity and resolution of this inelastic peak is better than in these previous works. The better resolution is due to a smaller modulation amplitude used in our work. The larger intensity may be ascribed to

the orientation of CH<sub>2</sub> elongations (linked to the alkyl chain tilting) relatively to the metallic plane electrode [99].

2. The second important structure appears at 134.3 mV (1083.2 cm<sup>-1</sup>) and can be attributed to C–C vibrations. This assignation is consistent with Raman data [100] and the peak magnitude is the same as in the 8 carbon atoms alkyldithiol SAM obtained by Wang *et al* [89].

3. The third important inelastic peak is observed at 187.9 mV (1515 cm<sup>-1</sup>) in our spectrum. We attribute it to  $\delta$ -s CH<sub>2</sub> vibration. The HREELS data give its energy at 180 mV (1451.7 cm<sup>-1</sup>). A comparable inelastic structure was observed at 180 mV as a very little peak by Wang *et al* [89] and as a CH<sub>2</sub> wagging vibration located at 170 mV by Kushmerik *et al* [88]. The intensity of the various CH<sub>2</sub> modes observed in these three IETS works depends on the alkyl chain lengths, but this intensity is not exactly proportional to the number of carbon atoms, and there exists a saturation trend [101].

4. The last characteristic peak is located at 242.9 mV (1960 cm<sup>-1</sup>). This peak has not been clearly assigned at the moment. Further experiments are in progress.

#### 4. Conclusion

In conclusion, we demonstrate that SAMs containing  $\pi$ -groups (phenyl, anthracene, pyrene, ethylenedioxythiophene, ethylenedioxyphenyl, thiophene, terthiophene and quaterthiophene) can be obtained by sequential grafting of alkyl chains (different chain lengths from 6 to 15 methylene groups) which are functionalized in a second step. For all the  $\pi$ -groups investigated here, we observe a rectification behavior in their current–density vs. voltage characteristics, which extends our preliminary work using phenyl and thiophene groups [51]. A simple analytical model is fitted on the experimental current–voltage curves to determine the position of the  $\pi$ -group molecular orbitals with respect to the electronic structures of the silicon substrate and the metal top electrode. The electronic structure of these molecular rectifying junctions can be calculated using a self-consistent tight-binding method. Comparing with the experimental data allows us to conclude that Fermi level pinning at the  $\pi$ -group/metal interface is mainly responsible for the observed behavior. It also explains why the rectification effect does not depend on the nature of the  $\pi$ -groups, albeit they have been chosen to have significant variations in their electronic molecular orbitals in vacuum.

We demonstrate that a MOS tunnel junction is a suitable test-bed for studying inelastic transport phenomena in organic self-assembled monolayers. For the eight-carbon atoms alkyl chain, the most important molecular vibrations are identified and compared with recent similar IETS investigations on metal surfaces and with IR, Raman and HREELS data. We observe that vibronic coupling in the organic tunnel monolayer are more intense than in the SiO<sub>2</sub> tunnel junctions. This would help in understanding more deeply the transport properties in hybrid silicon/molecular electronic devices.

#### References

- [1] ITRS, International technology roadmap for semiconductors (2002)

- [2] R Compano, L Molenkamp and D J Paul, *Technology roadmap for nanoelectronics*, European Commission, IST programme, Future and Emerging Technologies, Brussels (2000)
- [3] A Ulman, *An introduction to ultrathin organic films: From Langmuir–Blodgett to self-assembly* (Academic Press, Boston, 1991)
- [4] G J Ashwell, J R Sambles, A S Martin, W G Parker and M Szablewski, *J. Chem. Soc. Chem. Commun.* **19**, 1374 (1990)
- [5] N J Geddes, J R Sambles and A S Martin, *Adv. Mater. Opt. Electron.* **5**, 305 (1995)
- [6] A S Martin, J R Sambles and G J Ashwell, *Phys. Rev. Lett.* **70**, 218 (1993)
- [7] R M Metzger, B Chen, U Höpfner, M V Lakshmikantham, D Vuillaume, T Kawai, X Wu, H Tachibana, T V Hughes, H Sakurai, J W Baldwin, C Hosch, M P Cava, L Brehmer and G J Ashwell, *J. Am. Chem. Soc.* **119**, 10455 (1997)
- [8] D Vuillaume, B Chen and R M Metzger, *Langmuir* **15**, 4011 (1999)
- [9] T Xu, I R Peterson, M V Lakshmikantham and R M Metzger, *Angew. Chem. Int. Ed. Engl.* **40**, 1749 (2001)
- [10] R M Metzger, T Xu and I R Peterson, *J. Phys. Chem.* **B105**, 7280 (2001)
- [11] C P Collier, E W Wong, M Belohradsky, F M Raymo, J F Stoddart, P J Kuekes, R S Williams and J R Heath, *Science* **285**, 391 (1999)
- [12] C P Collier, G Mattersteig, E W Wong, Y Luo, K Beverly, J Sampaio, F Raymo, J F Stoddart and J R Heath, *Science* **289**, 1172 (2000)
- [13] A R Pease, J O Jeppesen, J F Stoddart, Y Luo, C P Collier and J R Heath, *Acc. Chem. Res.* **34**, 433 (2001)
- [14] Y Chen, G-Y Jung, D A A Ohlberg, X Li, D R Stewart, J O Jeppesen, K A Nielsen, J F Stoddart and R S Williams, *Nanotechnology* **14**, 462 (2003)
- [15] Y Chen, D A A Ohlberg, X Li, D R Stewart, R S Williams, J O Jeppesen, K A Nielsen, J F Stoddart, D L Olynick and E Anderson, *Appl. Phys. Lett.* **82**, 1610 (2003)
- [16] C N Lau, D R Stewart, R S Williams and M Bockrath, *Nano Lett.* **4**, 569 (2004)
- [17] D R Stewart, D A A Ohlberg, P A Beck, Y Chen, R S Williams, J O Jeppesen, K A Nielsen and J F Stoddart, *Nano Lett.* **4**, 133 (2004)
- [18] L A Bumm, J J Arnold, M T Cygan, T D Dunbar, T P Burgin, L Jones II, D L Allara, J M Tour and P S Weiss, *Science* **271**, 1705 (1996)
- [19] L A Bumm, J J Arnold, T D Dunbar, D L Allara and P S Weiss, *J. Phys. Chem.* **B103**, 8122 (1999)
- [20] C Kergueris, J P Bourgoin and S Palacin, *Nanotechnology* **10**, 8 (1999)
- [21] M A Reed, C Zhou, C J Muller, T P Burgin and J M Tour, *Science* **278**, 252 (1997)
- [22] C Kergueris, J P Bourgoin, S Palacin, D Esteve, C Urbina, M Magoga and C Joachim, *Phys. Rev.* **B59**, 12505 (1999)
- [23] J Reichert, R Ochs, D Beckmann, H B Weber, M Mayor and H v Löhneysen, *Phys. Rev. Lett.* **88**, 176804 (2002)
- [24] H B Weber, J Reichert, F Weigend, R Ochs, D Beckmann, M Mayor, R Ahlrichs and H v Löhneysen, *Chem. Phys.* **281**, 113 (2002)
- [25] J Chen, M A Reed, A M Rawlett and J M Tour, *Science* **286**, 1550 (1999)
- [26] J Chen, W Wang, M A Reed, A M Rawlett, D W Price and J M Tour, *Appl. Phys. Lett.* **77**, 1224 (2000)
- [27] M A Reed, J Chen, A M Rawlett, D W Price and J M Tour, *Appl. Phys. Lett.* **78**, 3735 (2001)
- [28] Z J Donhauser, B A Mantooth, K F Kelly, L A Bumm, J D Monnell, J J Stapleton, D W Price, A M Rawlett, D L Allara, J M Tour and P S Weiss, *Science* **292**, 2303 (2001)

- [29] G K Ramachandran, T J Hopson, A M Rawlett, L A Nagahara, A Primak and S M Lindsay, *Science* **300**, 1413 (2003)
- [30] M Bruening, E Moons, D Yaron-Marcovitch, D Cahen, J Libman and A Shanzer, *J. Am. Chem. Soc.* **116**, 2972 (1994)
- [31] R Cohen, S Bastide, D Cahen, J Libman, A Shanzer and Y Rosenwaks, *Opt. Mat.* **9**, 394 (1998)
- [32] R Cohen, N Zenou, D Cahen and S Yitzchaik, *Chem. Phys. Lett.* **279**, 270 (1997)
- [33] C Joachim, J K Gimzewski and A Aviram, *Nature (London)* **408**, 541 (2000)
- [34] F Schreiber, *Prog. Surf. Sci.* **65**, 151 (2000)
- [35] W C Bigelow, D L Pickett and W A Zisman, *J. Colloid Sci.* **1**, 513 (1946)
- [36] R Maoz and J Sagiv, *J. Colloid and Interface Sci.* **100**, 465 (1984)
- [37] J B Brzoska, N Shahidzadeh and F Rondelez, *Nature (London)* **360**, 719 (1992)
- [38] J B Brzoska, I Ben Azouz and F Rondelez, *Langmuir* **10**, 4367 (1994)
- [39] D L Allara, A N Parikh and F Rondelez, *Langmuir* **11**, 2357 (1995)
- [40] A N Parikh, D L Allara, I Ben Azouz and F Rondelez, *J. Phys. Chem.* **98**, 7577 (1994)
- [41] C Boulas, J V Davidovits, F Rondelez and D Vuillaume, *Phys. Rev. Lett.* **76**, 4797 (1996)
- [42] D Vuillaume, C Boulas, J Collet, G Allan and C Delerue, *Phys. Rev.* **B58**, 16491 (1998)
- [43] B Mann and H Kuhn, *J. Appl. Phys.* **42**, 4398 (1971)
- [44] E E Polymeropoulos and J Sagiv, *J. Chem. Phys.* **69**, 1836 (1978)
- [45] J Collet, O Tharaud, A Chapoton and D Vuillaume, *Appl. Phys. Lett.* **76**, 1941 (2000)
- [46] J Collet and D Vuillaume, *Appl. Phys. Lett.* **73**, 2681 (1998)
- [47] K M Roth, J S Lindsey, D F Bocian and W G Kuhr, *Langmuir* **18**, 4030 (2002)
- [48] K M Roth, A A Yasserli, Z Liu, R B Dabke, V Malinovskii, K-H Schweikart, L Yu, H Tiznado, F Zaera, J S Lindsey, W G Kuhr and D F Bocian, *J. Am. Chem. Soc.* **125**, 505 (2003)
- [49] W G Kuhr, A R Gallo, R W Manning and C W Rhodine, *Mat. Res. Soc. Bulletin* **29**, 838 (2004)
- [50] N P Guisinger, M E Greene, R Basu, A S Baluch and M C Hersam, *Nano Lett.* **4**, 55 (2004)
- [51] S Lenfant, C Krzeminski, C Delerue, G Allan and D Vuillaume, *Nano Lett.* **3**, 741 (2003)
- [52] C Petit, G Salace, S Lenfant and D Vuillaume, *Microelectronic Engineering* **80**, 398 (2005)
- [53] A Nitzan and M A Ratner, *Science* **300**, 1384 (2003)
- [54] Y Xue, S Datta and M A Ratner, *J. Chem. Phys.* **115**, 4292 (2001)
- [55] J K Tomfohr and O F Sankey, *Phys. Rev.* **B65**, 245105 (2002)
- [56] S N Yaliraki, A E Roitberg, C Gonzalez, V Mujica and M A Ratner, *J. Chem. Phys.* **111**, 6997 (1999)
- [57] W Tian, S Datta, S Hong, R Reifengerger, J I Henderson and C P Kubiak, *J. Chem. Phys.* **109**, 2874 (1998)
- [58] A Kahn, N Koch and W Gao, *J. Polymer Sci.: Part B: Polymer Phys.* **41**, 2529 (2003)
- [59] H Ishii, K Sugiyama, E Ito and K Seki, *Adv. Mat.* **11**, 605 (1999)
- [60] H Haick, M Ambrico, T Ligonzo and D Cahen, *Adv. Mat.* **16**, 2145 (2004)
- [61] A Vilan, J Ghabboun and D Cahen, *J. Phys. Chem.* **B107**, 6360 (2003)
- [62] A Vilan, A Shanzer and D Cahen, *Nature (London)* **404**, 166 (2000)

- [63] D Vuillaume, *J. Nanosci. Nanotech.* **2**, 267 (2002)
- [64] S Lenfant, D Guerin, F Tran Van, C Chevrot, S Palacin, J-P Bourgoin, O Bouloussa, F Rondelez, C Delerue and D Vuillaume, *J. Phys. Chem. B*, doi 10.1021/jp053510u
- [65] J G Simmons, *J. Appl. Phys.* **34**, 2581 (1963)
- [66] C Krzeminski, G Allan, C Delerue, D Vuillaume and R M Metzger, *Phys. Rev.* **B64**, 085405 (2001)
- [67] C Krzeminski, C Delerue and G Allan, *J. Phys. Chem.* **B105**, 6321 (2001)
- [68] O Gershewitz, M Grinstein, C N Sukenik, K Regev, J Ghabboun and D Cahen, *J. Phys. Chem.* **B108**, 664 (2004)
- [69]  $V_T$  is defined as the intercept between a linear fit of the current at high negative voltages and the zero current  $y$ -axis
- [70] I R Peterson, D Vuillaume and R M Metzger, *J. Phys. Chem.* **A105**, 4702 (2001)
- [71] L E Hall, J R Reimers, N S Hush and K Silverbrook, *J. Chem. Phys.* **112**, 1510 (2000)
- [72] W Schottky, *Naturwissenschaften* **26**, 843 (1938)
- [73] N F Mott, *Proc. Camb. Philos. Soc.* **34**, 568 (1938)
- [74] J Bardeen, *Phys. Rev.* **71**, 717 (1947)
- [75] A M Cowley and S M Sze, *J. Appl. Phys.* **36**, 3212 (1965)
- [76] J Tersoff, *Phys. Rev. Lett.* **52**, 465 (1984)
- [77] V Heine, *Phys. Rev.* **138**, 1689 (1965)
- [78] H Vazquez, R Oszwaldowski, P Pou, J Ortega, R Perez, F Flores and A Kahn, *Europhys. Lett.* **65**, 802 (2004)
- [79] G L Fisher, A V Walker, A E Hooper, T B Tighe, K B Bahnck, H T Skriba, M D Reinard, B C Haynie, R L Opila, N Winograd and D L Allara, *J. Am. Chem. Soc.* **124**, 5528 (2002)
- [80] A V Walker, T B Tighe, O M Cabarcos, M D Reinard, B C Haynie, S Uppili, N Winograd and D L Allara, *J. Am. Chem. Soc.* **126**, 3954 (2004)
- [81] A V Walker, T B Tighe, M D Reinard, B C Haynie, D L Allara and N Winograd, *Chem. Phys. Lett.* **369**, 615 (2003)
- [82] G L Fisher, A E Hooper, R L Opila, D L Allara and N Winograd, *J. Phys. Chem.* **B104**, 3267 (2000)
- [83] D R Jung and A W Czanderna, *Critical reviews in solid state and materials sciences* **191**, 1 (1994)
- [84] H Ahn and J E Whitten, *J. Phys. Chem.* **B107**, 6565 (2003)
- [85] X Crispin, V Geskin, A Crispin, J Cornil, R Lazzaroni, W R Salaneck and J L Brédas, *J. Am. Chem. Soc.* **124**, 8131 (2002)
- [86] P Fontaine, D Goguenheim, D Deresmes, D Vuillaume, M Garet and F Rondelez, *Appl. Phys. Lett.* **62**, 2256 (1993)
- [87] M Halik, H Klauk, U Zschieschang, G Schmid, C Dehm, M Schütz, S Maisch, F Effenberger, M Brunnbauer and F Stellacci, *Nature (London)* **431**, 963 (2004)
- [88] J G Kushmerick, J Lazorcik, C H Patterson, R Shashidhar, D S Seferos and G Bazan, *Nano Lett.* **4**, 643 (2004)
- [89] W Wang, T Lee, I Krestchmar and M A Reed, *Nano Lett.* **4**, 643 (2004)
- [90] A Pecchia, A Di Carlo, A Gagliardi, S Sanna, T Frauenheim and R Guttierrez, *Nano Lett.* **4**, 2109 (2004)
- [91] G Salace, C Petit and D Vuillaume, *J. Appl. Phys.* **91**, 5896 (2002)
- [92] C Petit and G Salace, *Rev. Sci. Instrum.* **74**, 4462 (2003)
- [93] J Lambe and R C Jacklevic, *Phys. Rev.* **165**, 821 (1968)
- [94] J Klein, A Leger, M Belin, D Dufourneau and M J L Sangster, *Phys. Rev.* **B7**, 2336 (1973)

- [95] C Petit, G Salace and D Vuillaume, *J. Appl. Phys.* **96**, 5042 (2004)
- [96] C Petit, G Salace and D Vuillaume, *Solid-State Electron.* **47**, 1663 (2003)
- [97] R C Jacklevic and J Lambe, *Phys. Rev. Lett.* **17**, 1139 (1966)
- [98] C Castiglioni, M Gussoni and G Zerbi, *J. Chem. Phys.* **95**, 7144 (1991)
- [99] J Kirtley and J T Hall, *Phys. Rev.* **B22**, 848 (1980)
- [100] M A Bryant and J E Pempterton, *J. Am. Chem. Soc.* **113**, 8284 (1991)
- [101] N M D Brown, R B Floyd and D G Walmsley, *J. Chem. Soc. Faraday, Trans II* **75**, 261 (1979)